

Article

Modeling Evaporation of Water Droplets as Applied to Survival of Airborne Viruses

Leonid A. Dombrovsky ^{1,2,*} , Alexander A. Fedorets ² , Vladimir Yu. Levashov ³,
Alexei P. Kryukov ⁴, Edward Bormashenko ⁵  and Michael Nosonovsky ^{2,6} 

¹ Joint Institute for High Temperatures, 17A Krasnokazarmennaya St., Moscow 111116, Russia

² Institute of Environmental and Agricultural Biology (X-BIO), University of Tyumen, 6 Volodarskogo St., Tyumen 625003, Russia; fedorets@utmn.ru (A.A.F.); nosonovs@uwm.edu (M.N.)

³ Institute of Mechanics of Moscow State University, 1 Michurinskiy Prosp., Moscow 119192, Russia; vyl69@mail.ru

⁴ Moscow Power Engineering Institute, 14 Krasnokazarmennaya St., Moscow 111250, Russia; kryukovap@mail.ru

⁵ Department of Chemical Engineering, Engineering Sciences Faculty, Ariel University, Ariel 407000, Israel; edward@ariel.ac.il

⁶ Mechanical Engineering, University of Wisconsin—Milwaukee, 3200 North Cramer St., Milwaukee, WI 53211, USA

* Correspondence: ldombro@yandex.ru; Tel.: +7-910-408-0186

Received: 16 August 2020; Accepted: 8 September 2020; Published: 10 September 2020



Abstract: Many viruses, such as coronaviruses, tend to spread airborne inside water microdroplets. Evaporation of the microdroplets may result in a reduction of their contagiousness. However, the evaporation of small droplets is a complex process involving mass and heat transfer, diffusion, convection and solar radiation absorption. Virological studies indicate that airborne virus survival is very sensitive to air humidity and temperature. We employ a model of droplet evaporation with the account for the Knudsen layer. This model suggests that evaporation is sensitive to both temperature and the relative humidity (RH) of the ambient air. We also discuss various mechanisms such as the effect of solar irradiation, the dynamic relaxation of moving droplets in ambient air and the gravitational sedimentation of the droplets. The maximum estimate for the spectral radiative flux in the case of cloudless sky showed that the radiation contribution to evaporation of single water droplets is insignificant. We conclude that at small and even at moderately high levels of RH, microdroplets evaporate within dozens of seconds with the convective heat flux from the air being the dominant mechanism in every case. The numerical results obtained in the paper are in good qualitative agreement with both the published laboratory experiments and seasonal nature of many viral infections. Sophisticated experimental techniques may be needed for in situ observation of interaction of viruses with organic particles and living cells within microdroplets. The novel controlled droplet cluster technology is suggested as a promising candidate for such experimental methodology.

Keywords: water droplets; evaporation; modeling; coronavirus survival; airborne transmission; droplet cluster

1. Introduction

The recent outbreak of the COVID-19 disease caused by the human coronavirus SARS-CoV-2 has attracted the attention of the research community to the mechanisms of virus transmission. It is widely accepted that coronavirus particles are transmitted not only by the so-called contact transmission (direct or indirect) or by large droplets generated by a close expiratory event (coughing, sneezing). As large droplets fall quickly due to gravity, this droplet transmission mode takes place upon close contact only.

On the contrary, small microdroplets with sizes on the order of dozens of microns are responsible for the airborne transmission (also referred to aerosol transmission) [1–4]. When a respiratory virus of concern only leads to disease with low severity, airborne precautions are not likely to be justified [5]. However, this is not the case for dangerous SARS-CoV-2. The observations confirm that there is a substantial probability that even normal speaking causes airborne virus transmission in confined environments [6]. At the same time, the conditions of virus infection outdoors are not obvious and should be studied in detail. The effect of environmental factors of the airborne transmission of viruses is sometimes underestimated [7]. Some experimental studies have demonstrated that transmission of viruses is strongly modulated by temperature and humidity of ambient air. However, the mechanism by which temperature and humidity alter transmission outcomes remains unclear [8,9].

It is interesting that numerous microdroplets in the atmosphere can transport microorganisms and viruses and play an important role in many biological processes including the long-distance migration of biological material and disease transmission. In natural environments, bioaerosols can be created by raindrops or sea sprays transferring bacteria and viruses from soil surface or sea water. Note that some metabolically active bacteria can survive airborne for many hours, and they have been detected in air at elevations as high as 20–70 km [10–12].

Viruses also use atmospheric aerosol particles to migrate for significant distances. Virus particles (virions) typically have submicron-scale size, therefore, they are much smaller than bacteria, which makes it difficult to observe them with the optical microscopy resolution. Thus, coronavirus particles have a spherical shape with the diameter of about 80 nm, and they are surrounded by a virus envelope made of a lipid bilayer, to which structural proteins of the membrane, envelope, and spikes are attached [13]. The coronavirus also has protein spikes up to 20 nm long, whose scanning electron microscope (SEM) images resemble a solar corona (hence the name “coronavirus”). The diameter of the virus particle, including the spikes is about 0.12 μm [14] (Figure 1).

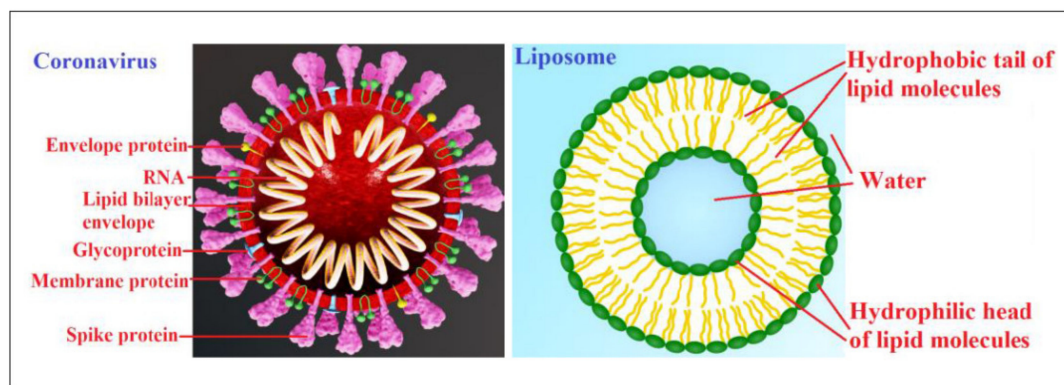


Figure 1. Schematic of an enveloped coronavirus and a liposome with a lipid bilayer membrane. Adopted from <https://en.wikipedia.org/wiki/Coronavirus> and <https://es.wikipedia.org/wiki/Liposoma>.

A major factor complicating the study of bioaerosols is that it is extremely difficult to observe airborne bacteria, and even more so, virus particles, in situ, because it is impossible to trace individual microdroplets in aerosols. However, we have recently suggested the droplet cluster technology, which allows the observation of isolated aerosol droplets for extended time spans (hours) and studying them with fluorescence microscopy [15]. Of course, direct observation of viruses and even assemblies of viruses [16] using conventional optics rather than an electron microscope is impossible. Therefore, we are talking about observing the transformation of proteins, as well as relatively large microorganisms under the influence of viruses in droplets with a diameter of several tens of microns.

The droplet cluster is a 2D array of microdroplets (10–100 μm diameter) levitating in an ascending gas (air mixed with vapor) flow over a locally heated layer of water. This fascinating phenomenon was discovered by Fedorets [17] and studied extensively not only by the authors of the present paper but also by other research groups. The milestones of this study include stabilization of the cluster managing

the cluster parameters that is important for the laboratory observations of biochemical processes in single droplets. In addition to [15,17], we refer to several basic publications [18–23] related to cluster management as applied to the observation of processes in the droplets. the droplets levitate at a height comparable with their radii, where the vertical component of the drag force is equilibrated by their own weight [24]. A cluster with any number (from one to hundreds) of monodisperse droplets can be generated and it tends to self-assemble into a hexagonally-ordered structure. the technology to control the number and size of droplets has been suggested and demonstrated by our group earlier including the ability to stabilize the cluster at relatively low temperatures (from 25 °C) [20], trace individual droplets for extended periods of time (hours), and observe micron-sized particles in droplets using the fluorescent microscopy [15].

In the present paper, we discuss the factors which affect the survival of airborne coronaviruses in small water droplets. the respiratory droplets contain dissolved salt with a mass fraction of about 0.01 as well as a small amount of proteins and pathogens [25]. However, it is assumed that the effect of this impurity and very small viruses or their aggregates on evaporation of water droplets is insignificant in contrast to that observed by evaporation of sea water droplets [26].

One can suggest that the virus do not survive if the droplet of water that carries it evaporates before the droplet contacts a potential victim of the virus. At least, this virus activity is expected to decrease strongly after complete evaporation of the droplet. Therefore, we focus on the effect of environmental conditions on the rates of evaporation and drying of droplets which carry the virus particles. the perspectives of studying bioaerosols in situ using the droplet cluster technology are also briefly discussed.

We consider only one aspect of the problem associated with the spread of a viral infection through the air. This study raises the important question of whether personal protective equipment (medical masks or respirators, and safety glasses) should be used outdoors. You can just sit on a park bench and people around you can be more than social distance. But this does not mean that you are completely safe, since viruses can be carried by micro-droplets of water. the gravitational settling of small droplets is very slow. These droplets can also evaporate slowly, especially in humid air and in cool weather. It is expected that understanding the settling and evaporation of small airborne water droplets will be helpful in some general guidelines for preventing dangerous outdoor behavior. As far as we know, there are no publications on this specific issue.

2. Evaporation of Airborne Microdroplets Carrying Viruses

Most viruses of respiratory diseases are transmitted by aerosol microdroplets. the effective control and prevention of these infectious diseases depends on the ability to prevent the airborne spreading, and in particular, to understand how microdroplet evaporation depends on the environmental conditions, such as the temperature and humidity of ambient air.

2.1. Environmental Factors Affecting Airborne Viruses

While it remains debated whether virus particles can survive on dry surfaces or in dry air, they clearly prefer water environment (Agranovski et al. [27] and Lewis [3]). the recent study of the SARS-CoV-2 stability in aerosols and on various surfaces [4,28,29] showed that the virus remained stable in aerosols for an extended time during the duration of the experiment. As far as surfaces of different materials, the virus was more stable on plastic and stainless steel than on copper and cardboard. This result is understandable from the notion that the virus needs moisture to survive, which can condense on the surface of some materials [30]. Note that viruses can survive on human skin and some household and contaminated surfaces [31–33]. At the same time, the virus does not survive, for example, on the surface of ordinary woven materials from cotton fibers. This is because viruses need moisture to survive. That is why we assume that the evaporation of microdroplets of water containing the virus implies the cessation of their activity.

Earlier studies have suggested that lipid-containing viruses (i.e., those covered by a lipid bilayer envelope membrane, which is the case with coronaviruses) are also more viable in moist air than in dry air [34]. The lipid bilayer is a self-assembled spherical structure made of amphiphilic lipid molecules due to hydrophobic interactions between these molecules in a water environment. A lipid bilayer is formed by molecules which have hydrophilic heads and hydrophobic tails. When subjected to a water environment, these molecules can self-assemble into complex structures such as micelles and liposomes (Figure 1). They are also known for complex thermodynamic behavior with liposomes undergoing phase transition between gel and liquid states and micelles subject to spontaneous micellization at concentrations and temperatures above critical values. It is not surprising that lipid-containing viruses prefer water environments.

The effect of environmental factors on the survival of airborne virus which can result to disease transmission via air has been studied by many groups. Harper [35] investigated survival of several viruses including influenza at different temperatures and relative humidity (RH) levels and concluded that the best survival was at low temperatures and low RH. Schaffer et al. [36] studied the effect of the relative humidity (RH) on the survival of airborne influenza and found maximum stability at low levels of RH. Zhao et al. [37] studied the survival of an aerosolized Gumboro virus at different temperatures and RH. They found that the long-distance transmission of airborne virus is more likely to occur at 20 °C than at 10 °C or 30 °C. Ijaz et al. [38] studied survival of airborne human coronavirus 229E under different temperatures and RH levels. The trends which they found were somewhat contradictory. Best survival conditions were at RH = 50% (half-life about 67.3 h at 20 °C and 102.5 h at 6 °C). At higher RH = 80% virus half-life was shortest at 20 °C and longest at 6 °C with the opposite trend at lower RH = 30%. They concluded that the rule that “lipid-containing viruses more viable in moist air (above 50% RH) than in dry air” is invalid for the coronavirus at low temperatures. Pyankov et al. [39] studied survival of the aerosolized MERS coronavirus in the ambient air under controlled laboratory conditions. The results obtained demonstrate that the virus decay was much stronger for hot and dry air scenario with only 4.7% survival over 60 min procedure. The effect of atmospheric conditions such as relative humidity and temperature of air on spreading of different influenza viruses was studied also by Kormuth et al. [40]. It was emphasized that, according to [41] seasonal influenza viruses cause yearly infection cycles that tend to peak in the winter in temperature regions during raining periods in tropical climates. Reche et al. [42] studied deposition rates of viruses and bacteria traveling for long distances with aerosols created by sea spray. They found that even in pristine environments, the downward flux of viruses was on the order of 10⁹ per m² per day and two orders of magnitude higher than the rates for bacteria. The highest relative deposition rates for viruses were associated with atmospheric transport from marine sources, while the deposition of bacteria was correlated with rains and Saharan dust intrusions. Virus deposition was correlated with aerosols of size less than 0.7 μm, which could travel longer distances, as opposed to larger aerosols typical for bacteria.

As far as the mechanisms of airborne virus inactivation, these are still not well understood. It has been suggested that droplet evaporation (dependent on both the temperature and humidity of ambient air) is the major factor affecting droplet viability, with a possible effect of increasing salts concentrations as droplet evaporates [26,43,44]. It has been also suggested that temperature is a factor in virus stability because rates of protein and nucleic acid inactivation increase with temperature, while RH controls evaporation, and, eventually droplet's size and concentration of chemical substances [45]. Coronaviruses are inactivated with heating at temperatures of 55–60 °C [46,47]. Virus particles are mesoscale objects with molecular masses on the order of 10⁶–10⁹ Da, which is much larger than the atomic mass, but much smaller than the Avogadro number, $N_A = 6.022 \times 10^{23} \text{ mol}^{-1}$. Thermal fluctuations play a significant role for the mesoscale objects, and it is not surprising that viruses prefer water environment, which serves as a thermal reservoir stabilizing their temperature and preventing denaturation of proteins.

The experimental data suggest that the humidity and temperature play a key role in the viability of airborne viruses, likely due to drying of microdroplets which bear these viruses. To evaluate factors

and mechanisms responsible for drying of microdroplets, we employed a model for the droplet motion and evaporation. According to [48], the droplets of initial diameter up to 50 μm have the highest infection probability. This will be taken into account in subsequent calculations.

2.2. Motion of Microdroplets in Ambient Air

Consider first the model problem for dynamic relaxation of a non-evaporating spherical droplet in the viscous air. In the case of immovable air, the droplet velocity is given by the following equation:

$$\frac{du}{dt} = -\frac{3C_D}{8a} \frac{\rho_{\text{air}}}{\rho_w} u^2$$

$$u(0) = u_0 \quad (1)$$

where u_0 is the initial velocity of the droplet, a is the droplet radius, and C_D is the drag coefficient. the droplet radius is suggested to be much smaller than the capillary length; thus, a droplet is considered as perfectly spherical. For the microdroplets under consideration, the Stokes flow regime takes place (when the Reynolds number $\text{Re} = 2\rho_{\text{air}}ua/\eta_{\text{air}} \ll 1$, η_{air} is the dynamic viscosity of air). In this case, $C_D = 24/\text{Re}$ and Equation (1) is reduced to $\tau \dot{u} = -u$ and immediately solved as $u = u_0 \exp(-t/\tau)$, with the relaxation time given by:

$$\tau = \frac{2}{9} \frac{\rho_w a^2}{\eta_{\text{air}}} \quad (2)$$

Substituting the values of droplet radius $a = 20 \mu\text{m}$ and air viscosity $\eta_{\text{air}} = 1.85 \cdot 10^{-5} \text{ Pa}\cdot\text{s}$ to Equation (2) yields $\tau = 5 \text{ ms}$. the coordinate of the droplet along the droplet trajectory is obtained by integrating the velocity as:

$$z = u_0 \tau (1 - \exp(-t/\tau)) \quad (3)$$

According to Equation (3), at $t = 2\tau$ the droplet is almost in dynamic equilibrium with air environment. In the case of $u_0 = 1 \text{ m/s}$, this equilibrium occurs at the very small distance of $z_* = u_0 \tau = 5 \text{ mm}$. the solution obtained indicates that the dynamic equilibrium takes place for the horizontal motion of a microdroplet in ambient air.

As to the vertical component of the droplet velocity, one should take into account the gravity, and the droplet will fall down even in the immovable air. It can be easily shown that the vertical velocity of the droplet increases with time as follows:

$$v(t) = g\tau(1 - \exp(-t/\tau)) \quad (4)$$

It is assumed here that the initial velocity $v(0) = 0$. Obviously, at a small relaxation time we obtain the constant "equilibrium" velocity $v = g\tau$ from Equation (4), and the total time of falling the droplet from the height h is equal to $t_* = h/(g\tau)$. This time may be comparable with the characteristic time of the droplet evaporation. Therefore, the vertical motion of evaporating water droplets should be taken into account in the general problem solution.

2.3. Modeling of Evaporation of Microdroplets

When a water droplet is placed in air not saturated by water vapor, evaporation prevails over condensation. However, droplet evaporation is a complicated process governed by interplay of combined mass and heat transfer, surface tension and other thermal effects. In order to calculate the time for droplet evaporation and temperature of the droplets, we use an evaporation model, based on the assumption that the Knudsen layer exists at the surface of the droplet. This allows coupling the kinetic theory of gases and the diffusion approach outside the Knudsen layer [49–52]. the evaporation model has shown a good agreement with the experimental data [53]. This model has been also successfully employed in recently published studies [23,26]. Note that the thickness of

the Knudsen layer is on the order of the mean free path of gas molecules (about 0.2 μm under ambient conditions), and the model is applicable for droplets of larger radii.

First, we assume that the temperature difference within the droplet is negligible, which is justified for small droplet. Following [23], consider the characteristic time scale, $\tau_{rel,t}$, of the thermal equilibration of small water droplets. This time scale may be roughly estimated from the equation $Fo = \alpha_w \tau_{rel,t} / a^2 = 1$, where $\alpha_w = k_w / (\rho_w c_w)$ is the thermal diffusivity of water and Fo is the Fourier number. Substituting $\alpha_w = 1.5 \cdot 10^{-7} \text{ m}^2/\text{s}$ and $a = 40 \text{ μm}$ yields $\tau_{rel,t} = 11 \text{ ms}$, which is much smaller than the characteristic time scales of thermal processes addressed in the paper. It means that the isothermal model for such water droplets is really applicable. In the case of some impurities, one can also assume that the mass diffusion process will lead to the uniform composition of small droplets.

The effect of the surface curvature on droplet evaporation is also neglected, since such an effect is significant only for submicron droplets. the dependency of the droplet temperature on time is obtained from the transient energy balance equation for a uniform droplet suspended in air:

$$\rho_w c_w \frac{dT}{dt} = \frac{1.5 Nu k_{air}}{a^2} (T_{air} - T) - 3 \frac{\dot{m} L_{ev}}{a}$$

$$T(0) = T_0 \tag{5}$$

where $Nu = 2ah/k_{air}$ is the Nusselt number for convective heat transfer from ambient air, h is the convective heat transfer coefficient, a is the radius of a droplet, \dot{m} is the mass rate of evaporation per unit of droplet’s surface, ρ_w and c_w are the density and specific heat capacity of water, L_{ev} is the latent heat of water evaporation, T_{air} is the air temperature at a distance from the droplet (outside the thermal boundary layer), k_{air} is the thermal conductivity of air. the first term in the right-hand side of Equation (5) characterizes the incoming heat flux, while the second term is the heat loss due to the evaporation. In the Stokes flow regime the problem is simplified. In addition, we do not take into account the effect of vapor blowing on the convective heat transfer. In this case, $Nu = 2$, and Equation (5) becomes:

$$\rho_w c_w \frac{dT}{dt} = \frac{3 k_{air}}{a^2} (T_{air} - T) - 3 \frac{\dot{m} L_{ev}}{a}$$

$$T(0) = T_0 \tag{6}$$

Note that the mass rate of evaporation is related to the derivative of the droplet radius. This gives us an additional differential equation for the droplet radius:

$$\rho_w \frac{da}{dt} = -\dot{m}$$

$$a(0) = a_0 \tag{7}$$

In the case of constant temperature of a droplet, Equation (6) gives the following expression for the evaporation flow rate:

$$\dot{m} = k_{air} (T_{air} - T) / (a L_{ev}) \tag{8}$$

This enables one to solve Equation (7) and obtain the known d-squared law ($d = 2a$ is the droplet diameter) [54]:

$$a^2 = a_0^2 - k_{air} t / \rho_w \tag{9}$$

It was shown in [55], that more realistic parabolic approximation of a quasi-steady temperature profile in the droplet (instead of the assumption of isothermal droplet) gives the so-called elliptic law instead of the d-squared law (9) for the time dependence of droplet size. the problem under consideration is far from the thermal equilibrium and Equation (8) is not applicable. In the present paper, we use much more sophisticated model for the isothermal droplet evaporation. This model is discussed below.

We should not also forget about the vertical motion of the droplet and calculation of the current vertical displacement of the droplet:

$$H(t) = g \int_0^t \tau(t) dt \tag{10}$$

The specific of the problem to be solved makes reasonable to consider the range of $H < H_*$, where H_* is the maximum difference in height between the source of infection and the face of potential victim. Under normal living conditions (indoors or outdoors), the value of H_* is about one meter. Therefore, in subsequent calculations, $H_* = 1$ m is taken. In this case, only those droplets containing the virus that are in the range of heights (from the source of infection) of $0 < H < 1$ m are considered dangerous.

The task is to calculate the time during which a droplet with viruses does not completely evaporate and, at the same time, is in a dangerous range of heights. In relation to the behavior of people sitting or walking outside, this minimum time allows one to estimate the distance that should be added to the accepted social distance in order to determine a truly safe distance between people. Of course, the safe distance depends on the relative speed of movement of people (and in the case of wind, on its speed and direction), since it is important not to be too early in the place of an infected person without a respirator (alas, being on the street, people, in many cases, do not wear a medical mask or respirator).

The coupled Equations (6) and (7) should be completed by an evaporation model for a single water droplet. According to the employed evaporation model, the vapor removal from the outer boundary of the Knudsen layer is due to diffusion. the value of the diffusion mass flow rate is calculated as follows:

$$\begin{aligned} \dot{m} &= \frac{Dp_e}{aR_{\text{air}}T_{\text{air}}} \ln\left(\frac{1 - \psi(T_{\text{air}})\varphi_e}{1 - \psi(T)\varphi_K}\right) \\ \psi(T) &= \frac{p_{\text{sat}}(T)}{p_e} \frac{M_w}{M_{\text{air}}} \end{aligned} \tag{11}$$

where D is the diffusion coefficient, p_e is the pressure of the gas mixture far from the droplet surface, φ_K and φ_e are the values of the RH at the outer boundary of the Knudsen layer and far from the droplet, respectively, R_{air} is the gas constant of air, $M_w = 18$ kg/kmol and $M_{\text{air}} = 29$ kg/kmol are the molar masses of water and air, p_{sat} is the pressure of saturated water vapor [56]. Equation (11) can be also written using the Spalding mass transfer number [54–58]. the saturated water pressure as a function of temperature can be obtained from the Antoine approximation [59] recommended by the NIST WebBook:

$$\lg p_{\text{sat}}(T) = 4.6543 - \frac{1435.264}{T - 64.848} \tag{12}$$

where T is in Kelvins and p_{sat} is in bars (10^5 Pa). the RH at the Knudsen layer boundary is further determined from the mass balance equation with the right-hand side taken from Equation (11):

$$f_{\text{ev}} \frac{p_{\text{sat}}(T)}{\sqrt{2\pi R_w T}} (1 - \varphi_K) = \frac{Dp_e}{aR_{\text{air}}T_e} \ln\left(\frac{1 - \psi(T_{\text{air}})\varphi_e}{1 - \psi(T)\varphi_K}\right) \tag{13}$$

The dimensionless coefficient f_{ev} in Equation (13) accounts for air in the Knudsen layer, and a numerical solution to the Boltzmann kinetic equation for evaporating of water droplets yields the value of $f_{\text{ev}} = 0.0024$ [52].

2.4. Numerical Results for Evaporation of Water Droplets

The following values of physical parameters are used in subsequent calculations: $D = 3 \cdot 10^{-5}$ m²/s, $R_w = 461.7$ J/(kg K), $R_{\text{air}} = 286.5$ J/(kg K), $p_{\text{air}} = 0.1$ MPa, $k_{\text{air}} = 0.026$ W/(m K), $\rho_w = 10^3$ kg/m³, $c_w = 4.18$ kJ/(kg K), $L_{\text{ev}} = 2.26$ MJ/kg. the calculations showed a strong effect of the air humidity on evaporation of small water droplets. For the variants of low or high RH, in which the droplets completely evaporate, only slightly moving down ($H < H_*$) under the action of gravity, the numerical

results are presented Figure 2. the same values of $T_0 = T_{air} = 27\text{ }^\circ\text{C}$ were used for all variants. Note that the value of the initial droplet temperature has an extremely weak effect on the calculation results, while the ambient temperature, like the air humidity, is an important parameter of the problem.

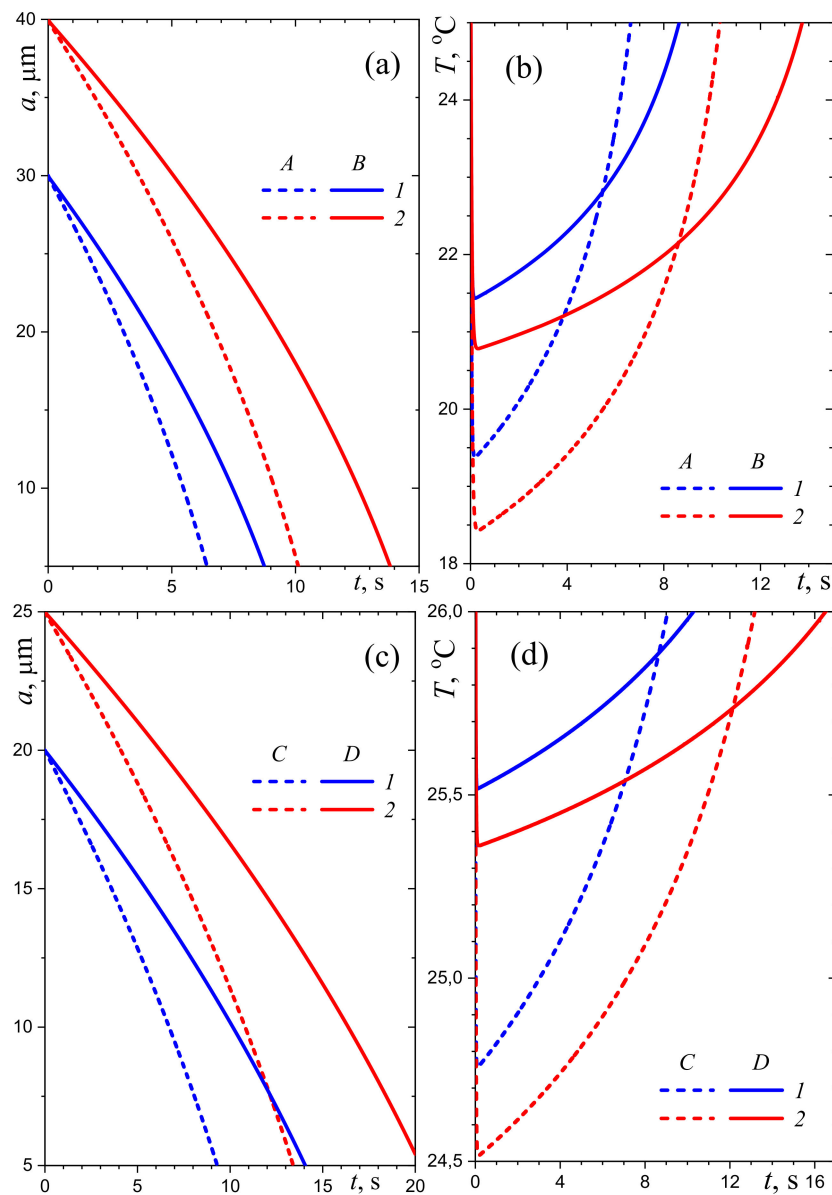


Figure 2. Time-dependency of the droplet radius and temperature (a,b) at low RH of air (A—20%, B—40%; 1— $a_0 = 30\text{ }\mu\text{m}$, 2— $40\text{ }\mu\text{m}$) and (c,d) at high RH of air (C—70%, D—80%; 1— $a_0 = 20\text{ }\mu\text{m}$, 2— $25\text{ }\mu\text{m}$); $T_{air} = 27\text{ }^\circ\text{C}$.

One can see in Figure 2b,d that at the beginning of the evaporation, when a droplet's radius decreases slowly, the evaporation results in a sharp decrease of droplet's temperature and this effect is especially pronounced in the case of low air humidity. After that the droplet is heated due to convective heat flux from ambient air. Such time dependences of temperature are explained by the large value of the latent heat of evaporation and are observed not only for small droplets, but also (and even to a greater extent) for thin films of polymer solutions [60].

At the beginning of evaporation, there is no effect of convective heat transfer on the droplet temperature and the time variation of the droplet radius is relatively slow. It means that one can use the following reduced equation for the droplet temperature:

$$\rho_w c_w \frac{dT}{dt} = -3 \frac{\dot{m}_0 L_{ev}}{a_0}$$

$$T(0) = T_0 \tag{14}$$

Obviously, the linear initial decrease of temperature T with time can be obtained using Equation (14) as it was done in [60]. the ambient temperature also has a significant effect on the evaporation of micro-droplets of water. To quantify this effect, it is sufficient to carry out calculations at a lower air temperature than those shown in Figure 2. the numerical results obtained at air temperature of $T_{air} = 17\text{ }^\circ\text{C}$ are shown in Figure 3.

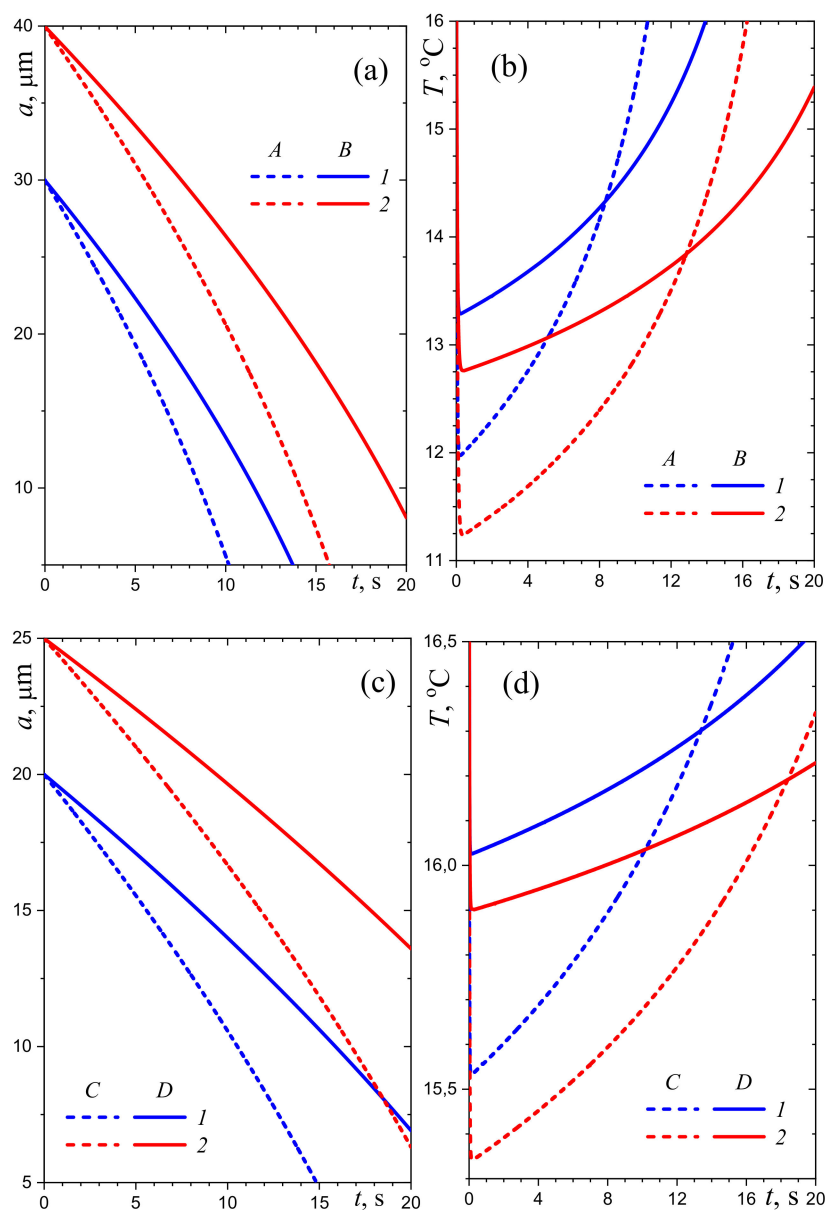


Figure 3. Time-dependency of the droplet radius and temperature (a,b) at low RH of air (A—20%, B—40%; 1— $a_0 = 30\ \mu\text{m}$, 2— $40\ \mu\text{m}$) and (c,d) at high RH of air (C—70%, D—80%; 1— $a_0 = 20\ \mu\text{m}$, 2— $25\ \mu\text{m}$); $T_{air} = 17\text{ }^\circ\text{C}$.

As expected, at lower air temperatures and the same relative humidity, water droplets evaporate much more slowly. As a result, water droplets with the same initial radius fall much faster. In particular, at RH = 40%, droplets with $a_0 = 40 \mu\text{m}$ pass the “critical height” without being able to completely evaporate (Figure 3a,b). At RH = 80%, water droplets with $a_0 = 25 \mu\text{m}$ behave in a similar way. Thus, gravitational settling partially compensates for the increase in the residence time of slowly evaporating droplets with viruses in a potentially dangerous zone.

It is of interest to generalize the numerical data for evaporating water droplets with an initial radii in the range from 10 to 40 μm in the form of the dependence of the maximum residence time, t_{max} , of water droplets (possibly containing viruses) at a dangerous altitude on two key parameters: temperature and relative humidity of ambient air. The calculated values of t_{max} for moderately warm and hot weather with not too high relative humidity of air are presented in Figure 4.

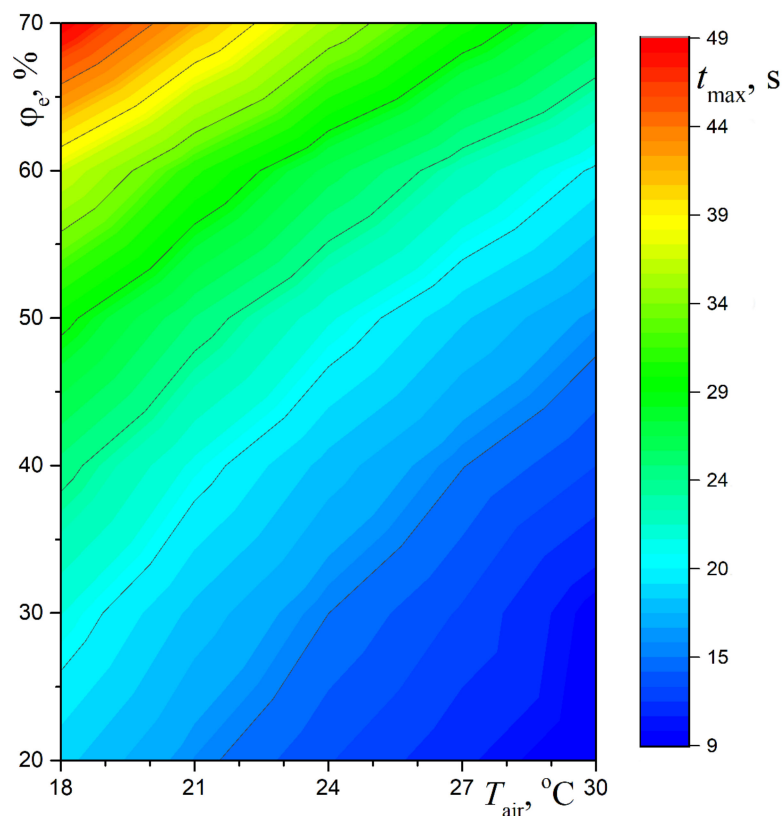


Figure 4. The maximum residence time of levitating microdroplets which may contain viruses.

It can be seen that the most dangerous infectious situation on the street, both for pedestrians and for people sitting on benches, for example, in squares or parks, occurs in the case of cool weather and high relative humidity of air. Of course, even at $t_{\text{max}} = 15 - 20 \text{ s}$ social distancing is clearly insufficient and it is highly desirable to use personal protective equipment such as medical masks and protective glasses.

Note that Figure 4 does not show the most dangerous areas of parameters, which are typical for summer in the Arctic regions (low temperature and very high humidity), as well as for the rainy season in tropical regions. The latter circumstance only reinforces the above conclusion regarding the use of personal protective equipment in cities and even small towns (not necessarily with a high density of crowds on the streets or in the parks).

It should be recalled that the above computational results are in good qualitative agreement with numerous observations and a typical seasonal nature of different viral infections. Some additional physical estimates confirming the possibility of applying the above-proposed relatively simple approach to solving the problem are given below.

It should be noted that the above calculations in some respects complement recent experimental studies related to prolonged exposure of virus-laden small droplets in air indoors, especially in hospitals where SARS-CoV-2 infected patients are treated [61,62]. It turns out that not only in a hospital setting, but also outdoors, especially when a large number of people are gathered, even simple medical masks, strongly recommended in [62], can significantly reduce the spread of infection.

As was found in recent work [63], aerosol air pollution increases the risk of infection and severe disease. Of course, as noted in [63], this may be due to the influence of polluted air on lung damage and a decrease in the body’s resistance. At the same time, the influence of the conditions of the airborne transmission of dangerous viruses cannot be ruled out. This question, like many other poorly studied effects of the ambient air properties, requires further research.

2.5. Effect of Solar Radiation

Many bioaerosols exist in the outside environment, where they can be subject to solar radiation. Here we consider small (almost transparent) groups of droplets, so the single scattering approximation can be used instead of the general problem of radiative heat transfer in a scattering medium [64]. This is different from the situation of a water mist, when the solar radiation is strongly absorbed due to the multiple scattering by weakly absorbing droplets, at least near the irradiated side of the water mist containing small droplets [65].

With the solar irradiation is taken into account, the energy balance equation for a single suspended droplet should include an additional term:

$$\rho_w c_w \frac{dT}{dt} = 0.75 \frac{\bar{Q}_a}{a} q_{rad} + \frac{3 k_{air}}{a^2} (T_{air} - T) - 3 \frac{\dot{m} L_{ev}}{a}$$

$$T(0) = T_0 \tag{15}$$

Here q_{rad} is the solar radiative flux at the earth surface integrated over the spectrum and $\bar{Q}_a(a)$ is the average efficiency factor of absorption for the droplet [64].

In order to estimate the contribution of the solar radiation relative to the convective heating of the droplet from air, we compare the first two terms in the right-hand part of Equation (15). For the upper estimate, we will consider the averaged spectrum of the solar radiation, similar to that of the blackbody at $T_{sol} = 6000$ K, assuming $q_{rad} = 1$ kW/m² at the Earth surface. the average efficiency factor of absorption is calculated as:

$$\bar{Q}_a(a) = \int_{\lambda_1}^{\lambda_2} Q_a(a, \lambda) I_{\lambda,b}(T_{sol}) d\lambda \bigg/ \int_{\lambda_1}^{\lambda_2} I_{\lambda,b}(T_{sol}) d\lambda \tag{16}$$

where $I_{\lambda,b}$ is the Planck’s function, and the limits of integration can be at the wavelengths $\lambda_1 = 0.3$ μm and $\lambda_2 = 6$ μm. Following [26], instead of the exact Mie theory [64–67] we use the following approximation for a semi-transparent droplet:

$$Q_a = \frac{4n}{(n + 1)^2} [1 - \exp(-4\kappa x)] \tag{17}$$

where n and κ are the spectral indices of refraction and absorption for water, and $x = 2\pi a/\lambda$ is the diffraction parameter of a droplet. the dependency of \bar{Q}_a on the droplet radius is presented in Figure 5. Small values obtained are due to water droplets transparency, which is caused by a very small value of the water absorption index in the visible spectral range [68]. For the same reason, the degree of the exponent in Equation (17) is significant only in the infrared part of the spectrum, which makes the dependency of \bar{Q}_a on the droplet radius almost linear.

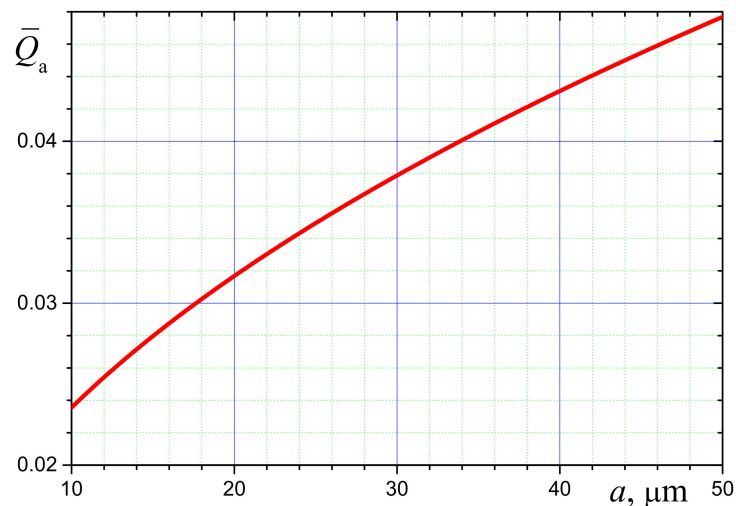


Figure 5. The average efficiency factor of absorption vs. the droplet radius.

As shown in Figure 5, the average efficiency factor of absorption is small, $\bar{Q}_a < 0.05$, for relevant droplet radii values. Assuming $a = 30 \mu\text{m}$ and for $\bar{Q}_a = 0.038$, we obtain the radiation term of the energy equation as $0.75\bar{Q}_a q_{\text{rad}}/a = 0.95 \text{ MW/m}^3$. This value is independent of the droplet temperature. Note that for a contaminated (non-transparent) droplet $\bar{Q}_a \approx 4n/(n+1)^2 = 0.98$ and the absorbed radiation power per volume is 24.5 MW/m^3 . To estimate the convective term in Equation (15), we assume the temperature difference between the droplet and air $T_{\text{air}} - T = 5 \text{ K}$ (see Figure 2b). In this case, we obtain $3k_{\text{air}}(T_{\text{air}} - T)/a^2 = 156 \text{ MW/m}^3$. A comparison with the radiation term shows that the contribution of the solar radiation is negligible.

3. A Promising Technology for Tracing Submicron Scaled Particles in Bioaerosols

In this section, we will describe the droplet cluster technology which can be used to trace individual aerosol droplets and which has already been discussed in [15]. In order to generate a levitating droplet cluster, a water layer with the thickness of 0.4 mm is typically used. A small area on the surface of the layer can be heated by a laser beam (Figure 6a).

This results in an air-water upward flow above the heated spot. There is an oversaturation of water vapor in the upward vapor-air flow. The oversaturation results in condensation of water droplets, often monodisperse (with the same size) usually with the diameters between $10 \mu\text{m}$ and $100 \mu\text{m}$. Since the vertical component of the aerodynamic drag force decreases with the distance from the water surface, the droplets tend to levitate at a low height (comparable with their radii) above the water surface, where their weight is equilibrated by the drag force. Besides the vertical component of the drag force, there is also a horizontal component directed towards the center of the heated spot, where the temperature is highest and the gas flow is most intense. Suspended droplets are driven towards the center. However, they do not coalesce, because there is also a repulsion force between the droplets, which is also aerodynamic in nature [23]. Consequently, droplets approach each other and settle (while levitating all at same height forming a monolayer) at a certain equilibrium distance from each other, where the drag towards the center is equilibrated by aerodynamic repulsion (Figure 6b). The droplets pack into a certain structure, and the most effective packing of many droplets is provided by a hexagonal (honeycomb) configuration (Figure 6c). The droplet cluster can be observed with an optical microscope.

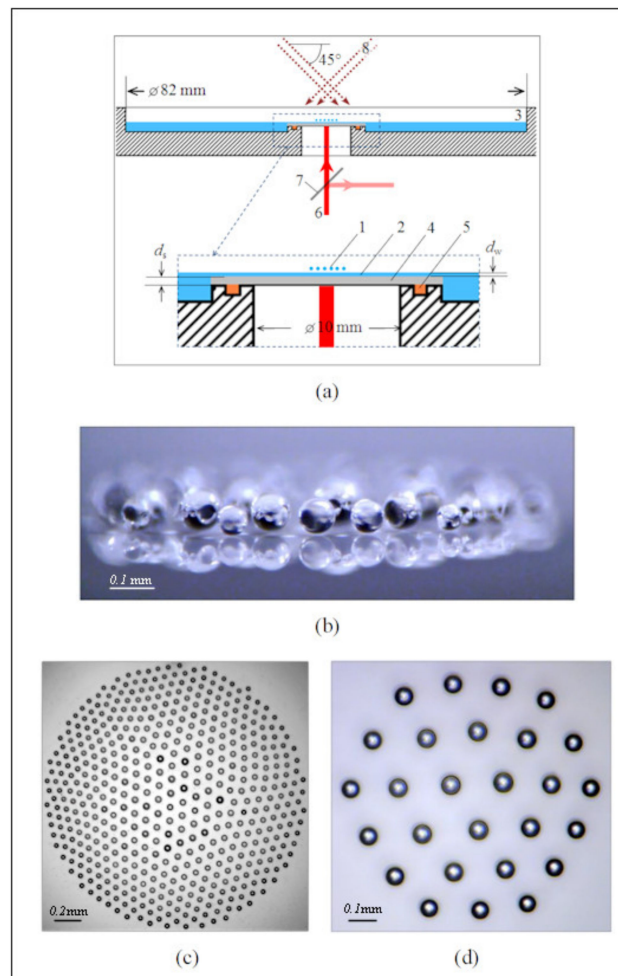


Figure 6. (a) the schematic of experimental setup for the droplet cluster (adopter from [19]), (b) side view of a cluster (adopted from [21]) and top views of a (c) large [15] and (d) small cluster.

Since the discovery of the droplet cluster, various methods to control their size and the distance between them have been developed. Clusters with any desired number of droplets, from a single droplet to hundreds of droplet can be generated (Figure 6d). While the condensation of droplets continues, their diameters increase, and eventually they will coalesce with the underlying water layer. Consequently, a typical life span of a droplet cluster is on the order of a minute. However, by irradiating and heating the droplets with the infrared radiation, the condensational growth can be suppressed [18,23]. It has been recently demonstrated in [23] that completely equilibrium small clusters containing several identical droplets can be produced and these clusters are stable during the extended periods of time sufficient for the laboratory biological study.

While high temperatures are not appropriate for experiments with biological materials, the droplet cluster can also be generated at much lower temperatures [20]. This makes the cluster suitable for biochemical analysis of living objects. A modified experimental setup to generate the room temperature droplet cluster included a separate volume of cold air just above the central part of water layer. Even moderate local heating of water surface is the most important factor to produce sufficiently large self-assembled levitating clusters of water droplets which are similar to those observed at higher temperatures.

In the past, we conducted an investigation of bioaerosols in stabilized droplet clusters with an Axio Zoom V16 fluorescence microscope (light source HXP 200C, filter set 38 HE, camera pso.edge 5.5, Zeiss, Jena, Germany) [15]. Microorganism cells (a green microalgae, *Chlorella vulgaris*, and of non-pathogenic *Escherichia coli*) bacteria were encapsulated into the droplets by ultrasound spreading (Figure 7).

We visualized treated bacterial cells with a permeabilized membrane employing a commercial staining kit containing DNA-intercalating dyes. The dyes allow to distinguish between the living and dead cells. The lightweight green fluorescence SYTO 9 (~400 Da) freely penetrates even through integral bacterial membrane, in contrast heavier red fluorescence PI (668 Da) is accumulated inside only through disordered plasma membrane. Membrane disordering was spectroscopically recorded as quenching of the green fluorescence since the SYTO 9 replaces by PI. The cells with undamaged membranes emit green light, while breaking of the cell membrane causes a chemical reaction and the color changes for red.

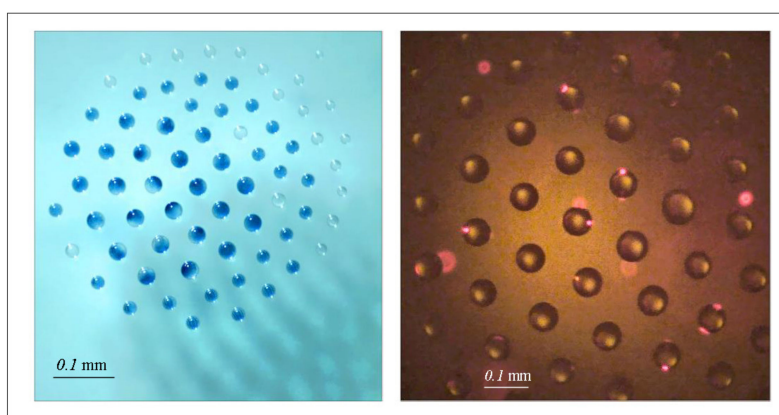


Figure 7. Photographs taken during bioaerosol experiments with the droplet cluster.

These results confirm that the droplet cluster is a feasible tool for the study of bioaerosols. However, the studies so far were conducted with cells. Virus particles are much smaller, and the direct in situ study of their behavior inside the suspended cluster droplets is not possible. At the same time, the observation of the transformation of some organic particles or cells under the influence of viruses attacking the larger particles seems to be quite real. These studies could provide an additional light on virus survival and their activity in microdroplets at various temperatures and other conditions.

4. Conclusions

Many viruses, such as the coronaviruses, tend to spread airborne inside water microdroplets. The disease transmission depends strongly on evaporation of microdroplets in ambient air. Drying of a small droplet is a complex process involving a combination of heat and mass transfer. The model suggested in the paper takes into account the interaction of different modes of heat transfer considering kinetics of evaporation. The computational study of the problem showed that the evaporation time of a small droplet is very sensitive to both the temperature and the relative humidity of ambient air. The sedimentation of evaporating particles under the action of gravity is also taken into account in the developed computational model. In some cases, it is the deposition of the droplets that determines the time of their presence in the layer of air that can pose a danger of airborne contamination. The results obtained enabled us to determine the most dangerous weather conditions for the virus outbreak. It was shown that low temperature and high humidity of air slow the evaporation of microdroplets and contribute to the long-term survival of the airborne virus. These findings are in good qualitative agreement with the experimental studies in laboratory conditions and also with the known seasonal nature of many viral infections. Sophisticated experimental techniques are needed for in situ observation of interaction of virus particles with relatively large micron-sized targets in microdroplets. The controlled droplet cluster is considered by the authors as a promising technology for such experimental studies.

Author Contributions: The original draft was prepared by L.A.D. and M.N. and revised by all authors. The calculations were conducted by L.A.D., the experimental data for droplet clusters were obtained by A.A.F. All authors have read and agreed to the published version of the manuscript.

Funding: This research received funding from the Russian Science Foundation, grant number 19-19-00076.

Conflicts of Interest: The authors declare no conflict of interest.

References

1. Stilianakais, N.I.; Drossinos, Y. Dynamics of infectious disease transmission by inhalable respiratory droplets. *J. R. Soc. Interface* **2010**, *7*, 1355–1366. [[CrossRef](#)] [[PubMed](#)]
2. Bourouiba, L. Turbulent gas clouds and respiratory pathogen emissions: Potential implications for reducing transmission of COVID-19. *J. Am. Med. Assoc.* **2020**, *323*, 1837–1838. [[CrossRef](#)] [[PubMed](#)]
3. Lewis, D. Is the coronavirus airborne? Experts can't agree. *Nature* **2020**, *580*, 175. [[CrossRef](#)] [[PubMed](#)]
4. Van Doremalen, N.; Bushmaker, T.; Morris, D.H.; Holbrook, M.G.; Gamble, A.; Williamson, B.N.; Tamin, A.; Harcourt, J.L.; Thornburg, N.J.; Gerber, S.I.; et al. Aerosol and surface stability of SARS-CoV-2 as compared with SARS-CoV-1. *N. Engl. J. Med.* **2020**, *362*, 1564–1567. [[CrossRef](#)]
5. Shiu, E.Y.C.; Leung, N.H.L.; Cowling, B.J. Controversy around airborne versus droplet transmission of respiratory viruses: Implication for infection prevention. *Curr. Opin. Infect. Dis.* **2019**, *32*, 372–379. [[CrossRef](#)]
6. Stadnytskyi, V.; Bax, C.E.; Bax, A.; Anfinrud, P. the airborne lifetime of small speech droplets and their potential importance in SARS-CoV-2 transmission. *Proc. Nat. Acad. Sci. USA* **2020**, *117*, 11875–11877. [[CrossRef](#)]
7. Tellier, R.; Li, Y.; Cowling, B.J.; Tang, J.W. Recognition of aerosol transmission of infectious agents: A commentary. *BMC Infect. Dis.* **2019**, *19*, 101. [[CrossRef](#)]
8. Lowen, A.C.; Steel, J. Roles of humidity and temperature in shaping influenza seasonality. *J. Virol.* **2014**, *88*, 7692–7695. [[CrossRef](#)]
9. Mittal, R.; Ni, R.; Seo, J.H. the flow physics of COVID-19. *J. Fluid Mech.* **2020**, *894*, F2. [[CrossRef](#)]
10. Després, V.R.; Huffman, J.A.; Burrows, S.M.; Hoose, C.; Safatov, A.S.; Buryak, G.; Fröhlich-Nowoisky, J.; Elbert, W.; Andreae, M.O.; Pöschl, U.; et al. Primary biological aerosol particles in the atmosphere: A review. *Tellus B Chem. Phys. Meteorol.* **2012**, *64*, 15598. [[CrossRef](#)]
11. Joung, Y.S.; Ge, Z.; Buie, C.R. Bioaerosol generation by raindrops on soil. *Nat. Commun.* **2017**, *8*, 14668. [[CrossRef](#)] [[PubMed](#)]
12. Wainwright, M.; Weber, P.K.; Smith, J.B.; Hutcheon, J.D.; Klyce, B.; Wickramasinghe, N.C.; Narlikar, J.V.; Rajaratnam, P. Studies on bacteria-like particles sampled from the stratosphere. *Aerobiologia* **2004**, *20*, 237–240. [[CrossRef](#)]
13. Lin, Y.; Yan, X.; Cao, W.; Wang, C.; Feng, J.; Duan, J.; Xie, S. Probing the structure of the SARS coronavirus using scanning electron microscopy. *Antivir. Ther.* **2004**, *9*, 287–289. [[PubMed](#)]
14. Almeida, J.D.; Berry, D.M.; Cunningham, C.H.; Hamre, D.; Hofstad, M.S.; Mallucci, L.; McIntosh, K.; Tyrrell, D.A.J. Virology: Coronaviruses. *Nature* **1968**, *220*, 650.
15. Fedorets, A.A.; Bormashenko, E.; Dombrovsky, L.A.; Nosonovsky, M. Droplet clusters: Nature-inspired biological reactors and aerosols. *Philos. Trans. R. Soc. A* **2019**, *377*, 20190121. [[CrossRef](#)]
16. Perlmutter, J.D.; Hagan, M.F. Mechanisms of virus assembly. *Annu. Rev. Phys. Chem.* **2015**, *66*, 217–239. [[CrossRef](#)]
17. Fedorets, A.A. Droplet cluster. *JETP Lett.* **2004**, *79*, 372–374. [[CrossRef](#)]
18. Dombrovsky, L.A.; Fedorets, A.A.; Medvedev, D.N. the use of infrared irradiation to stabilize levitating clusters of water droplets. *Infrared Phys. Technol.* **2016**, *75*, 124–132. [[CrossRef](#)]
19. Fedorets, A.A.; Dombrovsky, L.A. Generation of levitating droplet clusters above the locally heated water surface: A thermal analysis of modified installation. *Int. J. Heat Mass Transf.* **2017**, *104*, 1268–1274. [[CrossRef](#)]
20. Fedorets, A.A.; Dombrovsky, L.A.; Ryumin, P.I. Expanding the temperature range for generation of droplet clusters over the locally heated water surface. *Int. J. Heat Mass Transf.* **2017**, *113*, 1054–1058. [[CrossRef](#)]
21. Fedorets, A.A.; Frenkel, M.; Shulzinger, E.; Dombrovsky, L.A.; Bormashenko, E.; Nosonovsky, M. Self-assembled levitating clusters of water droplets: Pattern-formation and stability. *Sci. Rep.* **2017**, *7*, 1888. [[CrossRef](#)] [[PubMed](#)]
22. Fedorets, A.A.; Frenkel, M.; Bormashenko, E.; Nosonovsky, M. Small levitating ordered droplet clusters: Stability, symmetry, and Voronoi entropy. *J. Phys. Chem. Lett.* **2017**, *8*, 5599–5602. [[CrossRef](#)] [[PubMed](#)]

23. Dombrovsky, L.A.; Fedorets, A.A.; Levashov, V.Y.; Kryukov, A.P.; Bormashenko, E.; Nosonovsky, M. Stable cluster of identical water droplets formed under the infrared irradiation: Experimental study and theoretical modeling. *Int. J. Heat Mass Transfer* **2020**, *161*, 120255. [[CrossRef](#)]
24. Fedorets, A.A.; Dombrovsky, L.A.; Gabyshev, D.N.; Bormashenko, E.; Nosonovsky, M. An effect of external electric field on dynamics of levitating water droplets. *Int. J. Therm. Sci.* **2020**, *153*, 106375. [[CrossRef](#)]
25. Chaudhuri, S.; Basu, S.; Kabi, P.; Unni, V.R.; Saha, A. Modelling the role of respiratory droplets in COVID-19 type pandemics. *Phys. Fluids* **2020**, *32*, 063309. [[CrossRef](#)]
26. Dombrovsky, L.A.; Levashov, V.Y.; Kryukov, A.P.; Dembele, S.; Wen, J.X. A comparative analysis of shielding of thermal radiation of fires using mist curtains containing droplets of pure water or sea water. *Int. J. Therm. Sci.* **2020**, *152*, 106299. [[CrossRef](#)]
27. Agranovski, I.E.; Safatov, A.S.; Pyankov, O.V.; Sergeev, A.N.; Agafonov, A.P.; Ignatiev, G.M.; Ryabchikova, E.I.; Borodulin, A.I.; Sergeev, A.A.; Doerr, H.W.; et al. Monitoring of viable airborne SARS virus in ambient air. *Atmos. Environ.* **2004**, *38*, 3879–3884. [[CrossRef](#)]
28. Bhardway, R.; Agrawal, A. Likelihood of survival of coronavirus in a respiratory droplet deposited on a solid surface. *Phys. Fluids* **2020**, *32*, 061704. [[CrossRef](#)]
29. Kampf, G.; Todt, D.; Pfaender, S.; Steinmann, E. Persistence of coronaviruses on inanimate surfaces and their inactivation with biological agents. *J. Hosp. Infect.* **2020**, *104*, 246–251. [[CrossRef](#)]
30. Bormashenko, E.Y. *Wetting of Real Surfaces*, 2nd ed.; De Gruyter: Berlin, Germany, 2019.
31. Mukherjee, D.V.; Cohen, B.; Bovino, M.E.; Desai, S.; Whittier, S.; Larson, E.L. Survival of influenza virus on hands and fomites in community and laboratory settings. *Am. J. Infect. Control* **2012**, *40*, 590–594. [[CrossRef](#)]
32. Oxford, J.; Berezin, E.N.; Courvalin, P.; Dwyer, D.E.; Exner, M.; Jana, L.A.; Kaku, M.; Lee, C.; Letlape, K.; Low, D.E.; et al. the survival of influenza A(H1N1)pdm09 virus on 4 household surfaces. *Am. J. Infect. Control* **2014**, *42*, 423–425. [[CrossRef](#)] [[PubMed](#)]
33. Otter, J.A.; Donskey, C.; Yezli, S.; Douthwaite, S.; Goldenberg, S.D.; Weber, D.J. Transmission of SARS and MERS coronaviruses and influenza virus in healthcare settings: The possible role of dry surface contamination. *J. Hosp. Infect.* **2016**, *92*, 235–250. [[CrossRef](#)] [[PubMed](#)]
34. Ijaz, M.K.; Karim, Y.G.; Sattar, S.A.; Johnson-Lussenburg, C.M. Development of methods to study the survival of airborne viruses. *J. Virol. Meth.* **1987**, *18*, 87–106. [[CrossRef](#)]
35. Harper, G.J. Airborne micro-organisms: Survival tests with four viruses. *J. Hyg.* **1961**, *59*, 479–486. [[CrossRef](#)]
36. Schaffer, F.L.; Soergel, M.E.; Straube, D.C. Survival of airborne influenza virus: Effects of propagating host, relative humidity, and composition of spray fluids. *Arch. Virol.* **1976**, *51*, 263–273. [[CrossRef](#)]
37. Zhao, Y.; Aarnink, A.J.A.; Dijkman, R.; Fabri, T.; De Jong, M.C.M.; Koerkamp, P.W.G.G. Effects of temperature, relative humidity, absolute humidity, and evaporation potential on survival of airborne gumboro vaccine virus. *Appl. Environ. Microbiol.* **2012**, *78*, 1048–1054. [[CrossRef](#)]
38. Ijaz, M.K.; Brunner, A.H.; Sattar, S.A.; Nair, R.C.; Johnson-Lussenburg, C.M. Survival characteristics of airborne human coronavirus 229E. *J. Gen. Virol.* **1985**, *66*, 2743–2748. [[CrossRef](#)]
39. Pyankov, O.V.; Bodnev, S.A.; Pyankova, O.G.; Agranovski, I.E. Survival of aerosolized coronavirus in the ambient air. *J. Aerosol Sci.* **2018**, *115*, 158–163. [[CrossRef](#)]
40. Kormuth, K.A.; Lin, K.; Qian, Z.; Myerburg, M.M.; Marr, L.C.; Lakdawala, S.S. Environmental persistence of influenza viruses is dependent upon virus type and host origin. *mSphere* **2019**, *4*, e00552-19. [[CrossRef](#)]
41. Tamerius, J.; Nelson, M.I.; Zhou, S.Z.; Viboud, C.; Miller, M.A.; Alonso, W.J. Global influenza seasonality: Reconciling pattern across temperate and tropical regions. *Environ. Health Perspect.* **2011**, *119*, 439–445. [[CrossRef](#)]
42. Reche, I.; D’Orta, G.; Mladenov, N.; Winget, D.M.; Suttle, C.A. Deposition rates of viruses and bacteria above the atmospheric boundary layer. *ISME J.* **2018**, *12*, 1154–1162. [[CrossRef](#)] [[PubMed](#)]
43. Yang, W.; Marr, L.C. Mechanisms by which ambient humidity may affect viruses in aerosols. *Appl. Environ. Microbiol.* **2012**, *78*, 6781–6788. [[CrossRef](#)] [[PubMed](#)]
44. Linn, K.; Marr, L.C. Humidity-dependent decay of viruses, but not bacteria, in aerosols and droplets follows disinfection kinetics. *Environ. Sci. Technol.* **2020**, *54*, 1024–1032. [[CrossRef](#)] [[PubMed](#)]
45. Marr, L.C.; Tang, J.W.; Van Mullekom, J.; Lakdawala, S.S. Mechanistic insights into the effect of humidity on airborne influenza virus survival, transmission and incidence. *J. R. Soc. Interface* **2019**, *16*, 20180298. [[CrossRef](#)]

46. Duan, S.M.; Zhao, X.S.; Wen, R.F.; Huang, J.J.; Pi, G.H.; Zhang, S.X.; Han, J.; Bi, S.L.; Ruan, L.; Dong, X.P. Stability of SARS coronavirus in human specimens and environment and its sensitivity to heating and UV irradiation. *Biomed. Environ. Sci.* **2003**, *16*, 246–255.
47. Rabenau, H.F.; Cinatl, J.; Morgenstern, B.; Bauer, G.; Preiser, W.; Doerr, H.W. Stability and inactivation of SARS coronavirus. *Med. Microbiol. Immunol.* **2005**, *194*, 1–6. [[CrossRef](#)]
48. Chaudhuri, S.; Basu, S.; Saha, A. Analysing the dominant SARS-CoV-2 transmission routes towards an ab-initio SEIR model. *arXiv* **2020**, arXiv:2007.13596.
49. Kryukov, A.P.; Levashov, V.Y.; Sazhin, S.S. Evaporation of diesel fuel droplets: Kinetic versus hydrodynamic models. *Int. J. Heat Mass Transf.* **2004**, *47*, 2541–2549. [[CrossRef](#)]
50. Kryukov, A.P.; Levashov, V.Y.; Shishkova, I.N. Evaporation in mixture of vapour and gas mixture. *Int. J. Heat Mass Transf.* **2009**, *52*, 5585–5590. [[CrossRef](#)]
51. Levashov, V.Y.; Kryukov, A.P. Numerical simulation of water droplet evaporation into vapor–gas medium. *Colloid J.* **2017**, *79*, 647–653. [[CrossRef](#)]
52. Levashov, V.Y.; Kryukov, A.P.; Shishkova, I.N. Influence of the noncondensable component on the characteristics of temperature change and the intensity of water droplet evaporation. *Int. J. Heat Mass Transf.* **2018**, *127*, 115–122. [[CrossRef](#)]
53. Borodulin, V.Y.; Letushko, V.N.; Nizovtsev, M.I.; Sterlyagov, A.N. Determination of parameters of heat and mass transfer in evaporating drops. *Int. J. Heat Mass Transf.* **2017**, *109*, 609–618. [[CrossRef](#)]
54. Sirignano, W.A. *Fluid Dynamics and Transport of Droplets and Sprays*; Cambridge University Press: Cambridge, UK, 1999.
55. Dombrovsky, L.A.; Sazhin, S.S. A simplified non-isothermal model for droplet heating and evaporation. *Int. Commun. Heat Mass Transf.* **2003**, *30*, 787–796. [[CrossRef](#)]
56. Erbil, Y. Evaporation of pure liquid sessile and spherical suspended drops: A review. *Adv. Colloid Interface Sci.* **2012**, *170*, 67–86. [[CrossRef](#)] [[PubMed](#)]
57. Sazhin, S. *Droplets and Sprays*; Springer: London, UK, 2014.
58. Lefebvre, H.; McDonnell, V.G. *Atomization and Sprays*, 2nd ed.; CRC Press: New York, NY, USA, 2017.
59. Stull, D.R. Vapor pressure of pure substances. Organic and inorganic compounds. *Ind. Eng. Chem.* **1947**, *39*, 517–550. [[CrossRef](#)]
60. Dombrovsky, L.A.; Frenkel, M.; Legchenkova, I.; Bormashenko, E. Effect of thermal properties of a substrate on formation of self-arranged surface structures on evaporated polymer films. *Int. J. Heat Mass Transf.* **2020**, *158*, 120053. [[CrossRef](#)]
61. Liu, Y.; Ning, Z.; Chen, Y.; Guo, M.; Liu, Y.; Gali, N.K.; Sun, L.; Duan, Y.; Cai, J.; Westerdahl, D.; et al. Aerodynamic analysis of SARS-CoV-2 in two Wuhan hospitals. *Nature* **2020**, *582*, 557–560. [[CrossRef](#)]
62. Hu, J.; Lei, C.; Chen, Z.; Liu, W.; Hu, X.; Pei, R.; Su, Z.; Deng, F.; Huang, Y.; Sun, X.; et al. Airborne SARS-CoV-2 and the use of masks for protection against its spread in Wuhan, China. *Preprints* **2020**, 2020050464.
63. Contini, D.; Costabile, F. Does air pollution influence COVID-19 outbreaks? *Atmosphere* **2020**, *11*, 377. [[CrossRef](#)]
64. Dombrovsky, L.A.; Baillis, D. *Thermal Radiation in Disperse Systems: An Engineering Approach*; Begell House: New York, NY, USA, 2010.
65. Dombrovsky, L.A.; Solovjov, V.P.; Webb, B.W. Attenuation of solar radiation by water mist and sprays from the ultraviolet to the infrared range. *J. Quant. Spectr. Radiat. Transf.* **2011**, *112*, 1182–1190. [[CrossRef](#)]
66. Bohren, C.F.; Huffman, D.R. *Absorption and Scattering of Light by Small Particles*; Wiley: New York, NY, USA, 1983.
67. Mishchenko, M.I.; Travis, L.D.; Lacis, A.A. *Scattering, Absorption, and Emission of Light by Small Particles*; Cambridge University Press: Cambridge, MA, USA, 2002.
68. Hale, G.M.; Querry, M.P. Optical constants of water in the 200 nm to 200 μm wavelength region. *Appl. Opt.* **1973**, *12*, 555–563. [[CrossRef](#)]

